*Research supported in part by the U. S. Atomic Energy Commission and by the Air Force Office of Scientific Research, Office of Aerospace Research, United States Air Force, under Contract No. F44620-70-C-0028.

†On sabbatical leave from the Physics Department, University of Connecticut, Storrs, Conn. 06268. Participating guest, Lawrence Berkeley Laboratory.

[1]See E. J. McGuire [Phys. Rev. A 5, 1052 (1972); 3, 587 (1971)], where many of the earlier references could be found. Also W. Fink, R. C. Jopson, H. Marks, and C. D. Swift, Rev. Mod. Phys. 38, 513 (1966); W. Bambynek, B. Crasemann, F. W. Funk, H. U. Freund, H. Mark, C. D. Swift, R. E. Price, and P. V. Rao, Rev. Mod. Phys. 44, 716 (1972).

[2]V. O. Kostroun, M. H. Chen, and B. Crasemann, Phys. Rev. A 3, 533 (1971); 4, 1 (1971).

[3]See, for example, K. Omidvar, H. L. Kyle, and E. C. Sullivan, Phys. Rev. A 5, 1174 (1972).

[4]F. Herman and S. Skillman, *Atomic Structure Calculations* (Prentice-Hall, Englewood Cliffs, N. J., 1963).

[5]For example, R. Latter, Phys. Rev. 99, 510 (1955); J. C. Stewart and M. Rotenberg, *ibid.* 140, A1508 (1965).

[6]A. E. S. Green, D. L. Sellin, and A. S. Zachor, Phys. Rev. 184, 1 (1969).

[7]Y. Hahn and K. M. Watson, Phys. Rev. A 6, 548 (1972).

[8]N. F. Mott and H. S. W. Massey, *The Theory of Atomic Collisions* (Oxford U.P., Oxford, England, 1965), Chap. 16.

[9]Corrections for a relativistic impacting electron will be introduced later.

[10]E. T. Whittaker and G. N. Watson, *A Course of Modern Analysis* (Cambridge U.P., Cambridge, England, 1952), pp. 337–342.

PHYSICAL REVIEW A VOLUME 7, NUMBER 2 FEBRUARY 1973

Distorted-Wave Approximation and Its Application to the Differential and Integrated Cross Sections for Electron-Impact Excitation of the 2 ^1P State of Helium*

D. H. Madison and W. N. Shelton

Department of Physics, The Florida State University, Tallahassee, Florida 32306

(Received 15 December 1971; revised manuscript received 25 September 1972)

Theoretical results are given for the application of the distorted-wave approximation to electron-atom impact excitation for transitions from an L-S coupled initial state to an arbitrarily coupled final state. Expressions for the differential cross section and spin polarization of the emitted electrons are given for unpolarized electron beams incident upon unpolarized atoms. These results are applied to excitation of helium from its ground state to the $1s2p\ ^1P_1$ excited state for incident-electron energies between 26.5 and 300 eV. The results are compared with previous theoretical and experimental works. It is found that the distorted-wave calculation is superior to previous calculations in fitting the absolute magnitude and angular distribution of the experimental data. The improvement over the plane-wave calculations is greater at large angles, where the plane-wave approximations fail by several orders of magnitude.

I. INTRODUCTION

Until a few years ago, theories of electron-impact excitation were judged principally on their ability to predict integrated cross sections, while today there is an increasing emphasis on the correct prediction of the angular distributions as well. Recently there has also been an increasing interest in the spin polarization of the scattered electrons. This interest has been stimulated by the appearance of reliable experimental polarization data for unpolarized electron beams on unpolarized atomic targets. We can expect in the near future that theories of electron-impact excitation will be required to predict not only correct integrated and differential cross sections, but also correct angular distributions of electron spin polarization. It seems likely that those theories which predict incorrect spin polarization, or which yield no information of this type, can be expected to be of decreasing importance.

For the past several years many calculations have been made for inelastic electron-atom scattering cross sections using the Born[1,2] and other related plane-wave approximations.[3–10] These approximations give fairly good integrated cross sections, at high energy, for allowed transitions. The shape of the small-angle differential cross sections is reasonably good for allowed transitions provided the momentum transfer is small and the incident energy is sufficiently high.[8,11] However, the angular range over which the Born approximation gives approximately correct results decreases with increasing incident-electron energy. At a given incident-electron energy, the breakdown at large angles occurs rapidly once it has begun, so that an error of many orders of magnitude is quite common. As for the plane-wave exchange approximations, there is no evidence that any of them give even qualitatively correct angular distributions at

any energy, for either allowed or forbidden transitions. The failure of the plane-wave exchange approximations is seen most clearly for transitions in which the direct excitation mode is forbidden, such as the $1\,^1S$-$2\,^3P$ transition for helium.[12,13]

An additional defect of the plane-wave theories is that they predict zero spin polarization for the electrons emitted following scattering of an unpolarized electron beam on unpolarized target atoms.

Although the distorted-wave (DW) approximation was used by Massey and co-workers to treat the electron-scattering problem as early as the 1930's, it has been only recently that a resurgence of interest in this approximation has taken place. This is due mainly to the appearance of modern computing machinery capable of properly carrying out the DW approximation, and to the recent availability of good angular distribution data which make the failure of the plane-wave approximations obvious. One reason for the relative lack of interest in the DW approximation in the period 1940–1960 was that further approximations were necessary for computational convenience, and these approximations resulted in integrated cross sections which exceeded the experimental values by an even greater margin than did the plane-wave results.

In the DW approximation, the incident electron is taken to be elastically scattered by the initial-state atomic potential. If the excitation of the atom is through the direct process, the incident electron makes a transition to a state in which it is being elastically scattered by the final-state atomic potential. If the excitation of the atom is through the exchange process, the incident electron is captured into a bound state of the atom, while one of the initially bound electrons is ejected into an elastic-scattering state. In each case, the transition between the initial and final elastic-scattering states is calculated by a perturbationlike method. This procedure is to be contrasted with the one followed in the plane-wave approximations, which take the initial and final free-electron states to be plane waves and thus ignore the presence of the atom altogether in this part of the calculation. (For further discussion of the plane-wave versus DW approximation, see the fifth and following paragraphs of Sec. IV.)

Until very recently, little theoretical work had been done to develop a complete DW theory treating the multiparticle aspects of the electron-atom scattering problem. Some recent DW work was done by Sawada *et al.*,[14] but the detailed atomic structure was not considered. The most thorough previous effort in this direction was made by the present group for the excitation of rare-gas atoms.[15] A disadvantage of the latter work was that the atomic wave functions were expressed in a j-j coupling scheme using fractional parentage coefficients that are not widely tabulated. There exists a need for a general theory applicable to any atom developed in a coupling scheme appropriate for the atomic problem and in terms of coefficients readily available. In Sec. II such a theory is given for transitions from an L-S coupled initial atomic state to an arbitrarily coupled final state. The theory is easily extendable to arbitrary coupling schemes for the initial state, and to mixed configuration wave functions. General expressions for the differential cross section and spin polarization of the emitted electron are given. Section III contains the application of the theory to the excitation of helium from its ground state to the $1s2p\,^1P_1$ excited state, and the conclusions are in Sec. IV.

II. THEORY

The problem to be considered here is inelastic electron-atom scattering. The Hamiltonian for such a process is given by[16]

$$H = H_{\rm at} + T_0 + V_a = H_{\rm at'} + T_0 + V_b \ . \tag{1}$$

The Hamiltonian for the initial state of the n-electron atom is $H_{\rm at}$, with the prime indicating the final state; T_0 is the kinetic energy operator for the free electron whose coordinate is labeled $\vec{r}_0$, and $V_a(V_b)$ is the potential influencing the free electron in the incident (exit) channel. Since only atomic excitation will be considered, $H_{\rm at}$ and $H_{\rm at'}$ should be equal, and V_a and V_b should be equal. This distinction is made to allow for the fact that it may be desirable to choose these operators unequal when performing a calculation using self-consistent potentials.

If $V_b^s(0)$ is defined to be the spherical average of the interaction of the free electron with the atomic electrons in the exit channel (i.e., the negative of the electrostatic potential of the spherically averaged electronic charge distribution of the final atomic state), the T matrix in the DW approximation with full allowance for exchange symmetries is given by[15]

$$\begin{aligned} T_{ba} = \langle \phi_b^{(-)}(0)\psi_{J_B M_B}(1\cdots n)\left|\sum_{i=1}^{n}\frac{2}{r_{i0}} - V_b^s(0)\right| \\ \times \psi_{J_A M_A}(1\cdots n)\phi_a^{(+)}(0)\rangle - n\langle \phi_b^{(-)}(0) \\ \times \psi_{J_B M_B}(1\cdots n)\left|\sum_{i=1}^{n}\frac{2}{r_{i0}} - V_b^s(0)\right| \\ \times \psi_{J_A M_A}(0\cdots n-1)\phi_a^{(+)}(n)\rangle \ . \end{aligned} \tag{2}$$

The first term of (2) is the direct amplitude since the outgoing electron is the same as the incoming electron, and the second term is the exchange amplitude since the outgoing electron was originally in the atom. The properly antisymmetrized initial (final) atomic wave function is $\psi_{J_A M_A}(\psi_{J_B M_B})$,

the elastic-scattering wave function in the incident (exit) channel is $\phi_a(\phi_b)$, and r_{i0} is the distance between the electron whose coordinate is $\vec{r}_i$ and the free electron. The superscripts + (−) indicate satisfaction of the usual outgoing (incoming) wave boundary conditions. The elastic-scattering wave functions (DW's) are calculated on the potential

$$U_{a(b)} = -2Z/r_0 + V^s_{a(b)}(0) + V^R_{a(b)}(0) . \quad (3)$$

Here Z is the nuclear charge and V^R allows for the inclusion of relativistic (e.g., spin-orbit) and other small terms. Although these terms are not of significance for a light atom such as helium, we allow for their presence so that the results will be applicable to electron scattering on heavy atoms.

In order that a multiparticle expression such as (2) be evaluated, some specific assumptions about the form and orthogonality of the atomic wave functions must be made. The assumptions made here are the following.

(i) The atomic wave functions are suitable combinations of single-particle wave functions obtained in the central field model. The initial and final atomic states differ by one single-particle wave function. The initial-state wave function is assumed to be L-S coupled, and the final-state wave function is assumed to be arbitrarily coupled.

(ii) The bound-state single-particle wave functions are assumed to be mutually orthonormal. It can be seen that imposition of this orthogonality requirement alone results in several exchange terms. However, if the requirement that the bound-state single-particle wave functions be orthogonal to the free-state wave functions is imposed, all the exchange terms except one vanish. This orthogonality requirement was imposed to make the calculation tractable.

Assuming the above orthogonality requirements are satisfied, (2) reduces to

$$T_{ba} = n\langle \phi_b^{(-)}(0)\psi_{J_B M_B}(1\cdots n)\,|\,2/r_{n0}\,|\,\psi_{J_A M_A}(1\cdots n) \times \phi_a^{(+)}(0)\rangle - n\langle \phi_b^{(-)}(0)\psi_{J_B M_B}(1\cdots n)\,|\,2/r_{n0}\,| \times \psi_{J_A M_A}(0\cdots n-1)\phi_a^{(+)}(n)\rangle . \quad (4)$$

By making a partial-wave expansion of the distorted waves and exploiting the angular momentum properties of the system, it can be shown that[17]

$$T_{ba} = \sum_{lsj} \hat{j}\, C(J_A\, j J_B\,;\, M_A,\, M_B - M_A,\, M_B)\beta^{l m m_b m_a}_{sj}(\vec{k}_b, \vec{k}_a) . \quad (5)$$

The summation is performed for all the possible angular momenta transferred to the atom

$$\vec{j} = \vec{J}_B - \vec{J}_A .$$

This transferred angular momenta is composed of a spin part (s) and an orbital part (l). The symbol $C(j_1 j_2 j_3;\, m_1,\, m_2,\, m_3)$ is a Clebsch-Gordan coefficient,[18] $\hat{f} \equiv (2f+1)^{1/2}$, $\vec{k}_a$ ($\vec{k}_b$) is the initial (final) wave number of the free electron, m_a (m_b) is the spin projection of the free electron initially (finally) with $m = M_B - M_A + m_b - m_a$, and

$$\beta^{l m m_b m_a}_{sj}(\vec{k}_b, \vec{k}_a) = \sum_{\substack{l_a j_a m_1 \\ l_b j_b}} 4\pi I^{lsj}_{l_b j_b l_a j_a} i^{l - l_a - l_b}\, \hat{l}\hat{s}\hat{j}_b\; C(l_b s_b j_b\,;\, m_1 - m,\, m_b,\, m_b + m_1 - m) C(l_a s_a j_a\,;\, m_1,\, m_a,\, m_1 + m_a) \times C(j_b j j_a\,;\, m_1 + m_b - m,\, m - m_b + m_a,\, m_1 + m_a)\, X(l_a s_a j_a\,;\, l_b s_b j_b\,;\, lsj)\, Y^{m_1 *}_{l_a}(\theta_{k_a}\phi_{k_a})\, Y^{m_1 - m}_{l_b}(\theta_{k_b}\phi_{k_b}) . \quad (6)$$

Here X is a Fano coefficient,[19] $Y^{m_1}_{l_1}(\theta\phi)$ is a spherical harmonic, and s_a (s_b) is the initial (final) spin of the free electron. The radial integral is

$$I^{lsj}_{l_b j_b l_a j_a} = \frac{4\pi}{k_a k_b} \int r_n\, dr_n \int r_0\, dr_0 \chi_{l_b j_b}(k_b, r_0) \times \chi_{l_a j_a}(k_a, r_n) G^{sj}_{l l_b l_a}(r_0, r_n) . \quad (7)$$

where $\chi_{l_a j_a}(k, r)$ is the radial component of the partial-wave expansion of the incident-channel DW. The DW depends on j as well as l since we are allowing for relativistic effects (such as the spin-orbit term). The relativistic effects are important for heavy atoms. The angular-momentum properties of the atomic matrix elements are contained in the radial function G. The evaluation of G depends upon the form and coupling scheme of the atomic wave functions and involves lengthy angular momentum algebra. Using the wave functions assumed above, a straightforward, but tedious, calculation gives

$$G^{sj}_{l l_b l_a}(r_0, r_n) = \sum_{\substack{\alpha_P S_P L_P \\ \alpha_n l_n \alpha'_n l'_n}} \sum_{\{y\}} i^{l - l_n - l'_n} \hat{J}_A \hat{L}\hat{L}'\hat{l}_n\hat{l}'_n\, n\langle \alpha_P S_P L_P,\, \alpha'_n l'_n | \}\, \alpha' L' S' \rangle \langle \alpha_P S_P L_P,\, \alpha_n l_n | \}\, \alpha L S \rangle$$

$$\times R_C[O_C \rightarrow L'S']\, W(L'lL_P l_n; Ll'_n)\Big(\hat{s}_b \hat{l}_a \hat{l}_b \hat{l}^{-1}\, W(L'lSJ_A; LJ_B) C(l_a l_b l; 0,0,0) C(l_n l'_n l; 0,0,0)$$

$$\times I_l(r_0)\, \frac{\delta(r_n - r_0)}{r_n^2}\, \delta_{s0} - \hat{s}\hat{S}\hat{S}'\hat{l}\hat{j}\, W(S_P s_b S' s; S s_a) X(LlL'; SsS'; J_A j J_B) \sum_K (-)^K \hat{K}^2$$

$$\times W(l_n l_b l'_n l_a; Kl) C(l'_n K l_a; 0,0,0) C(l_n K l_b; 0,0,0) g_K(r_n, r_0) U_{l'_n}(r_n) U_{l_n}(r_0)\Big). \quad (8)$$

The first term in (8) results from the direct part of (4), and the second term results from the exchange part. The symbol W is a Racah coefficient,[20] L and S are the total orbital and spin angular momentum quantum numbers of the initial atomic wave function, and l_n (l'_n) is the single-particle quantum number of the transition orbit in the incident (exit) channel. The symbol $R_C[O_C \rightarrow L'S']$ represents all the angular momentum coefficients necessary to recouple the other coupling scheme of the final atomic wave function into an L'-S' basis, and the set $\{y\}$ represents all the quantities that need to be summed over for the recoupling. The quantity $\langle \alpha_P S_P L_P,\ \alpha_n l_n | \} \alpha LS \rangle$ is a coefficient of fractional parentage,[21,22] with $L_P S_P$ the total orbital and spin angular momentum of the parent and α_p, α_n, and α any additional quantum numbers necessary to describe the particular states completely. The sum over $\alpha_P S_P L_P \alpha_n l_n \alpha'_n l'_n$ is performed for all parents common to the initial and final atomic wave functions. The symbol U_{l_n} ($U_{l'_n}$) designates the atomic single-particle radial wave function in the incident (exit) channel, and the radial multipole factor g_K is defined by

$$g_K(r_n, r_0) = [2/(2K+1)]\, r_<^K / r_>^{K+1}, \quad (9)$$

where $r_<$ ($r_>$) is the smaller (larger) of r_n and r_0. The radial function in the direct term of (8) is

$$I_l(r_0) = \int r^2 U_{l'_n}(r)\, g_l(r, r_0)\, U_{l_n}(r)\, dr. \quad (10)$$

This function is referred to as the form factor.

In terms of the T matrix, the differential cross section for unpolarized beams incident upon unpolarized targets is given by

$$\frac{d\sigma}{d\Omega} = \frac{1}{16\pi^2}\, \frac{k_b}{k_a}\, \hat{J}_A^{-2} \hat{s}_a^{-2} \sum_{\substack{M_A M_B \\ m_a m_b}} |T_{ba}|^2. \quad (11)$$

Insertion of the form of T_{ba}, (5), into the above yields

$$\frac{d\sigma}{d\Omega} = \frac{1}{16\pi^2}\, \frac{k_b}{k_a}\, \frac{\hat{J}_B^2}{\hat{J}_A^2 \hat{s}_a^2} \sum_{j m m_b m_a} \Big| \sum_{ls} \beta_{sj}^{l m m_b m_a} \Big|^2. \quad (12)$$

Note that there is no interference between the terms representing different total angular momentum transferred to the atom (j), while there is interference between the different orbital and spin (l, s) contributions to a given j value.

The spin polarization $\vec{P}$ of an emitted particle is defined to be the expectation value of its spin operator. It can be shown that if an incident beam is unpolarized, only the component of $\vec{P}$ perpendicular to the plane $\vec{k}_a \times \vec{k}_b$ will be nonvanishing. If the z axis is chosen along $\vec{k}_a$ and the y axis along $\vec{k}_a \times \vec{k}_b$, β becomes a function of the angle θ between $\vec{k}_a$ and $\vec{k}_b$, and the polarization of the emitted electrons becomes[17]

$$P_y(\theta) = \left(\sum_{\substack{ss'll' \\ j m m_a m_b}} [(s_b - m_b)(s_b + m_b + 1)]^{1/2}\, \mathrm{Im}(\beta_{sj}^{l m m_b m_a} \beta_{s'j}^{l' m+1 m_b+1 m_a *}) \right) \left(s_b \sum_{\substack{ss'll' \\ j m m_a m_b}} \beta_{sj}^{l m m_b m_a} \beta_{s'j}^{l' m m_b m_a *} \right)^{-1}. \quad (13)$$

The spin polarization results from the fact that β is a complex number with a nonzero imaginary part. This imaginary contribution arises from the imaginary part of the radial DW's. Any free-state wave function whose partial-wave radial component is real in our phase convention, such as a plane wave, gives no spin polarization for the emitted electrons for the case considered here (i.e., unpolarized electron beams incident on unpolarized target atoms). This means, for example, that the Born approximation predicts zero spin polarization for this case.

III. EXCITATION OF THE $2\,^1P$ STATE OF HELIUM

The excitation of helium from the $1s^2\,1\,^1S$ ground state to the $1s2p\,2\,^1P_1$ excited state by electron impact has been the object of considerable experimental and theoretical investigation.[8,23,24] In spite of the considerable effort consumed in these prior studies, agreement between theory and experiment is still poor in many regions. The previous theoretical works have relied primarily on calculating direct excitation by means of the Born approximation,[1] and exchange excitation through

various Ochkur–Bonham-like relations.[4,6] A sampling of the present status of agreement between experiment and theory would be the following.

For differential scattering cross sections, Vriens *et al.*[25] found departures from the Born approximation in the shape of their small-angle ($5^\circ \leq \theta \leq 15^\circ$) experimental cross sections for energies less than 200 eV. This observation was supported by the work of Kim and Inokuti.[26] The small-angle theoretical cross sections calculated from very accurate generalized oscillator strengths are larger than the recent absolute differential cross section measurements of Chamberlain *et al.*[27] over the entire energy range. Truhlar *et al.*[8] found qualitative agreement between the shape of their experimental differential cross sections and their Born–Ochkur-like calculations in the range $10^\circ \leq \theta \leq 40^\circ$ for energies between 34 and 81.6 eV. Their theoretical cross sections fall much faster than the data for $\theta > 40^\circ$. The absolute magnitude of their theoretical cross sections was too large for small angles and too small for large angles. Recently Hidalgo and Geltman[28] compared the results of their Coulomb-projected Born approximation with the large-angle data of Opal and Beaty[29] at 82 and 200 eV and found improvement over the Born approximation at large angles.

Integrated Born cross sections obtained from Kim and Inokuti's[26] generalized oscillator strengths are much larger than the experimental integrated cross sections of Jobe and St. John[30] for incident energies under 200 eV. The integrated cross sections of the Coulomb-projected Born approximation were larger than those of the Born approximation in this energy range.

A. Wave Functions

One of the requirements imposed on the wave functions in Sec. II was that all the bound- and free-state single-particle wave functions be mutually orthogonal. In practice, it is difficult to obtain accurate wave functions and still meet all the orthogonality requirements. Ideally, one would wish to obtain self-consistent Hartree–Fock wave functions for the bound and free electrons in the incident channel, and then perform a similar calculation for the exit channel, keeping these new self-consistent wave functions orthogonal to the ones obtained in the incident channel. The difficulties of such a project can be appreciated by studying the elastic-scattering work of La Bahn and Callaway.[31] The large amount of computer effort required for the evaluation of the exchange integral dictated that the formation of the DW's represent a minor part of the calculation. For this reason, the decision was made to calculate the DW's on spherically averaged potentials obtained from available self-consistent bound-state wave functions.

The question that arises immediately is whether the accuracy of the bound-state wave functions is more important to the calculation than orthogonality between the bound- and free-state wave functions. The orthogonality requirement could be met exactly by calculating all the bound- and free-state wave functions on a single potential. Naturally such a procedure would not yield accurate bound-state wave functions. In the opposite extreme, one could use the best available Hartree–Fock bound-state wave functions for the incident and exit channels, and then calculate the DW's on the respective atomic potentials without regard to the orthogonality requirement. Another possibility is that the most desirable state might lie intermediate between these two extremes. Since there was no *a priori* way of knowing the answers to these questions, various possibilities were examined. The different methods used for obtaining the single-configuration, L-S coupled wave functions were as follows.

(a) Exact orthogonality and poorest bound-state wave functions (HG): for this case the bound-state and free-state wave functions for both channels were calculated as eigenfunctions of a single atomic potential. The potential used was that of the ground state of helium obtained from the self-consistent Hartree–Fock–Slater program of Herman and Skillman.[32]

(b) Orthogonality within channels and good bound-state wave functions (H): in this case the bound-state and free-state wave functions for a given channel were calculated as eigenfunctions of the atomic potential for that channel. The atomic potentials for the respective channels were obtained from the Herman and Skillman[32] program.

(c) Orthogonality between channels and better bound-state wave functions (FG): for this case the ground and excited bound-state wave functions were calculated in the frozen-core approximation using Fischer's[33] Hartree–Fock program. In the frozen-core approximation, the $1s$ wave function of the excited state is chosen to be identical to the $1s$ wave function of the ground state. The DW's for both channels were calculated as eigenfunctions of the atomic potential obtained from the ground-state wave function. (This makes the DW's orthogonal.) Figure 1 shows this atomic potential.

(d) Worst orthogonality for the free-state wave functions but best bound-state wave functions (F): for this case the bound-state wave functions were calculated in their respective channels using Fischer's[33] program. The distorted wave for each channel was then calculated on the potential given by the self-consistent wave functions for that channel. Orthogonality is not obtained between the bound- and free-state wave functions within a channel since the bound-state wave functions are not

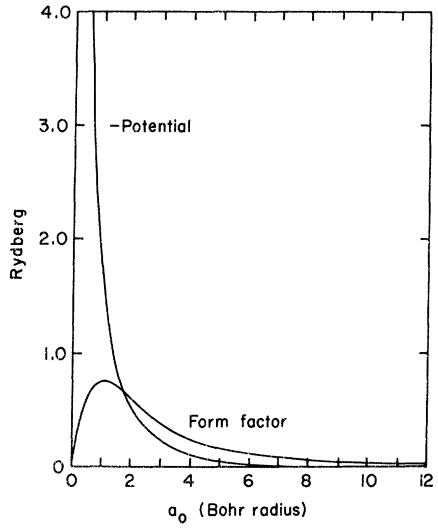

FIG. 1. Negative of the atomic potential and the inelastic form factor for the excitation of the $2\,^1P$ state of helium obtained from the FG wave functions.

eigenfunctions of the spherically averaged self-consistent Hartree–Fock potential.

B. Numerical Procedure

The calculation was performed on a CDC 6400 computer. The code was checked against plane-wave calculations for scattering from hydrogen[11,34] and helium. Noumerov's method[35] was used to solve the radial equation in the evaluation of the DW's. The DW's were formed on a mesh whose step size ($0.00176a_0$) was doubled after each block of 40 points until the number of points per lobe of the wave function reached a minimum number, and beyond this point a constant step size was used. The minimum usable number of points per lobe for the wave function was found to be 13, but a larger number is desirable and was generally used. Simpson's method[36] was used to evaluate the radial overlap integrals. Typical run time for an incident energy of 29 eV was about 15 min, increasing up to almost 2 h for an incident energy of 300 eV. The time required for a given energy is not appreciably affected by the number of scattering angles calculated.

C. Direct Case

In the evaluation of the direct amplitude, the DW's are integrated against the form factor [see Eqs. (7) and (8)]. The DW's must therefore be known out to a radius where the form factor effectively vanishes. The point where the form factor effectively vanishes also determines the number of partial waves required. This can be seen from the following consideration. The radius at which a partial wave first acquires an appreciable value moves out from the origin with increasing partial-wave order. The limit on the number of partial waves that need to be considered is reached when additional partial waves are effectively zero over the range of finiteness of the form factor. This limiting number increases with increasing energy of the incident electron.

For a l transfer of 1 unit, the form factor (10) falls off like K/r^2 for large r, where K is a constant proportional to the electric dipole matrix element taken between the initial and final bound-state wave functions. The form factor obtained from the bound-state wave functions FG of Sec. III A is shown in Fig. 1. The unfortunate fact that the form factor falls off so slowly requires integration of each partial wave out to a large radius, and also requires the evaluation of many partial waves. For incident energies of 29–81 eV this maximum radius was taken to be $288a_0$, but for energies in the range 100–300 eV this value was reduced to $144a_0$ to provide enough points per lobe for the more rapidly varying wave functions. The errors involved in the calculation will be examined in Sec. III F.

The total number of partial waves required for the evaluation of the direct amplitude was about 17 for an incident energy of 29.2 eV, and 200 for an incident energy of 300 eV. However, it was not necessary to numerically calculate the contributions from all the partial waves. Higher partial waves that are effectively zero over the range of the atomic potential ($\sim 40a_0$) approximate spherical Bessel functions. At the large radii where these partial waves begin to acquire a finite value, the form factor will have already fallen to its asymptotic value of K/r^2. Under these circumstances we were able to obtain an analytic expression for the direct part of (7). At 29.2 eV 13 partial waves were calculated numerically, and at 300 eV 80 were calculated numerically. Higher partial waves were calculated analytically.

D. Exchange Case

The exchange case is free of the numerically troublesome long-range interaction problem appearing in the direct case for allowed transitions. However, an independent double integration must be carried out for each contributing pair of partial waves so that the exchange case is considerably more time consuming for the computer. Since a DW is integrated against a bound-state wave function for the exchange case, the radial integration may be terminated at the radius where the bound-state wave function effectively goes to zero. This occurs at about $12a_0$ for the ground state and about $40a_0$ for the excited state. The total number of partial waves needed for evaluation of the exchange

amplitude was 13 for an incident energy of 29.2 eV and 42 for an incident energy of 300 eV.

E. Results

1. Differential Cross Section

Figures 2–5 compare the results of this calculation with the experimental and theoretical work of Truhlar *et al.*[8] for incident energies of 34, 44, 55.5, and 81.63 eV. Each figure gives the direct, exchange, and total differential cross sections from this work and total differential cross sections from Truhlar *et al.* The DW calculations are labeled HG, H, FG, and F. The curve labeled HG resulted from using the poorest wave functions, but ones that ensured exact orthogonality; H resulted from using good wave functions and orthogonality within channels; FG resulted from using better wave functions and orthogonality between channels; and F resulted from using the best wave functions and the poorest orthogonality. (For a more complete description, see Sec. III A.) The experimental points are "absolute" in the sense that they were normalized to the integral cross sections of Jobe and St. John.[30] The solid curves are various Born and Born–Ochkur–Bonham-like results calculated using the Kim and Inokuti set of generalized oscillator strengths. The abbreviations are: B, Born approximation; O and OP, Ochkur approximation (prior and post forms); BOR and BORP, Born–Ochkur–Rudge approximation (prior and post forms); and BTKF, Born-transferred Kang–Foland approximation. (For a more complete description of these approximations see Ref. 8.)

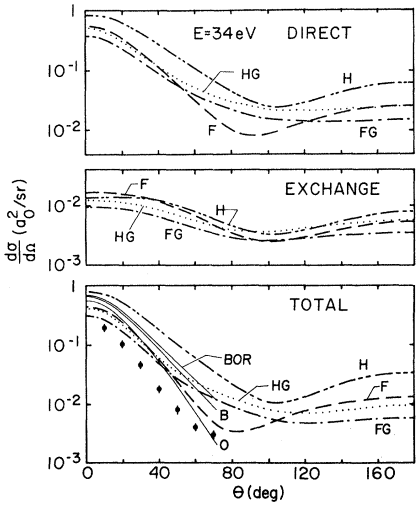

FIG. 2. Theoretical and experimental differential cross sections for electron-impact excitation of the $2\,^1P$ state of helium at an incident energy of 34 eV. The curves labeled H, HG, F, and FG are distorted-wave calculations, and the curves labeled B, O, and BOR are plane-wave calculations. The labels are described in the text in Sec. III E 1. The experimental data (heavy dots) is that of Truhlar *et al.*

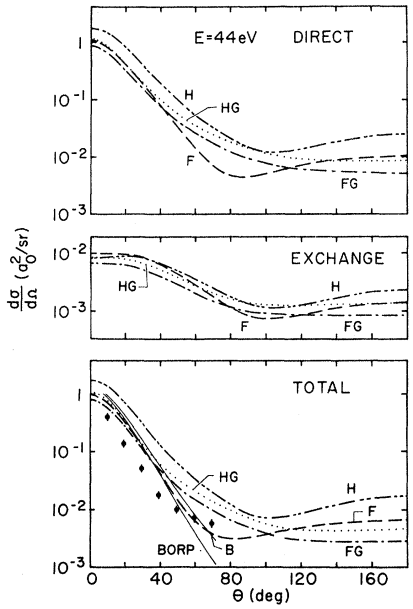

FIG. 3. Same as Fig. 2 except here the energy is 44 eV.

Examination of these four figures reveals that the FG curve is superior for predicting the absolute magnitude of the cross section for small angles and gives the best over-all fit to the data. The only notable exception to this rule occurs at 34 eV where F better predicts the shape of the

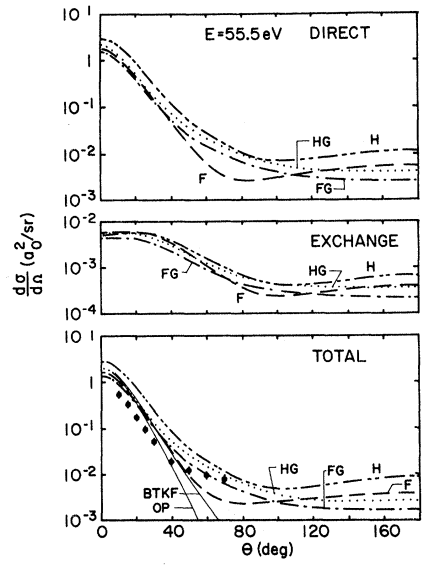

FIG. 4. Same as Fig. 2 except here the energy is 55.5 eV.

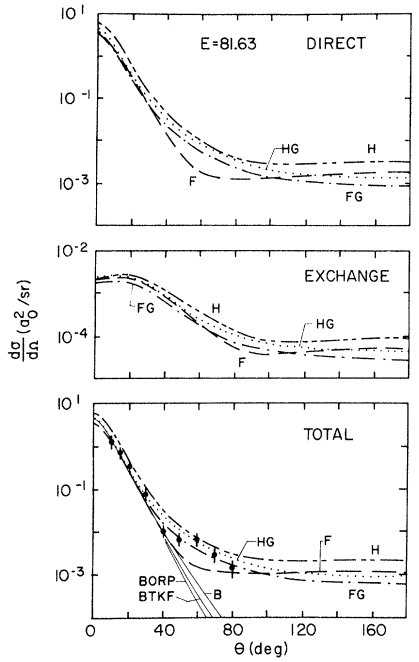

FIG. 5. Same as Fig. 2 except here the energy is 81.63 eV.

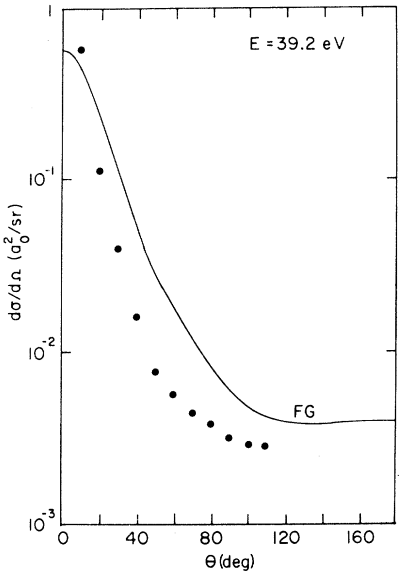

FIG. 7. Same as Fig. 6 except here the energy is 39.2 eV.

data. At 81.63 eV, FG is within the experimental error at practically every experimental point. The DW calculations represent a marked improvement over the Born calculations for fitting the large-angle experimental data, and with the exception of H, give lower small-angle cross sections.

Mazeau[37] has also taken low-energy data, but over a larger angular range $10° \leq \theta \leq 110°$. In Figs. 6–8, we compare his data with the DW calculations FG for incident-electron energies of 29.2, 39.2, and 48.2 eV. Crooks and Rudd[38] have recently performed absolute measurements over an even larger angular range, $10° \leq \theta \leq 150°$, at 50

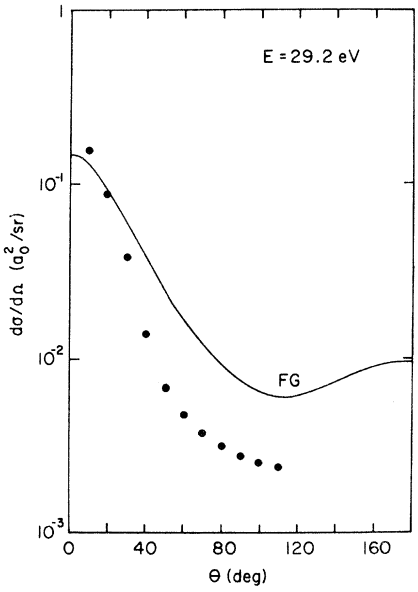

FIG. 6. Comparison of the distorted-wave calculation FG with the experimental results (heavy dots) of Mazeau for the excitation of the $2\,^1P$ state of helium at 29.2 eV.

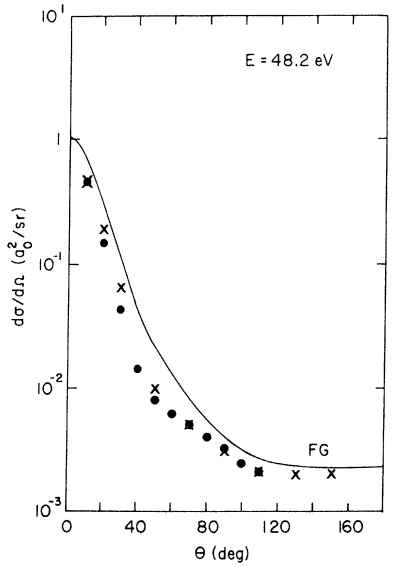

FIG. 8. Comparison of the distorted-wave calculation FG with the experimental results of Mazeau (dots) for the excitation of the $2\,^1P$ state of helium at 48.2 eV. Also shown are the experimental results of Crooks and Rudd (crosses) taken at 50 eV.

and 100 eV. Their data for 50 eV are included with the results for 48.2 eV in Fig. 8. It is seen that the FG calculation fits the larger-angular-range data as well as it fits the corresponding data of Figs. 2–5 which extend over a more limited angular range.

Figures 9–14 compare experimental and theoretical differential cross sections for incident-electron energies between 100 and 300 eV. The experimental data extending to 150° at 100 eV are those of Crooks and Rudd.[38] The small-angle data at each of these energies are that of Vriens *et al.*[25] normalized to the absolute measurements of Chamberlain *et al.*[27] (The normalization for incident energies of 175 and 225 eV was obtained from Fig. 16.) The solid curve labeled B in these figures is the Born approximation calculated using Kim and Inokuti's generalized oscillator strengths. The remaining curves are DW calculations, with the abbreviations as before. It is seen that the FG calculation gives very good agreement with the 100-eV data of Crooks and Rudd over the entire angular range, and also gives the best fit to the small-angle data of Vriens *et al.* in the energy region

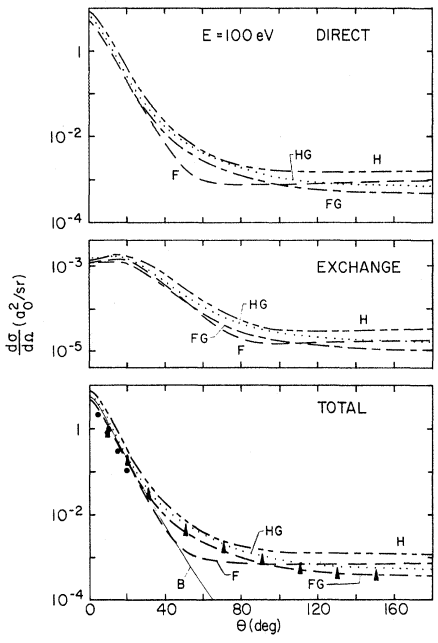

FIG. 9. Theoretical and experimental differential cross sections for electron-impact excitation of the $2\,^1P$ state of helium at an incident energy of 100 eV. The curves labeled H, HG, F, and FG are distorted-wave calculations and B is the Born approximation. A description of the distorted-wave labels is contained in Sec. III E 1. The experimental data are that of Vriens *et al.* (dots) and Crooks and Rudd (solid triangles). The distorted-wave curves F and FG are identical to within plotting accuracy in the direct and total cross sections for $\theta < 25°$.

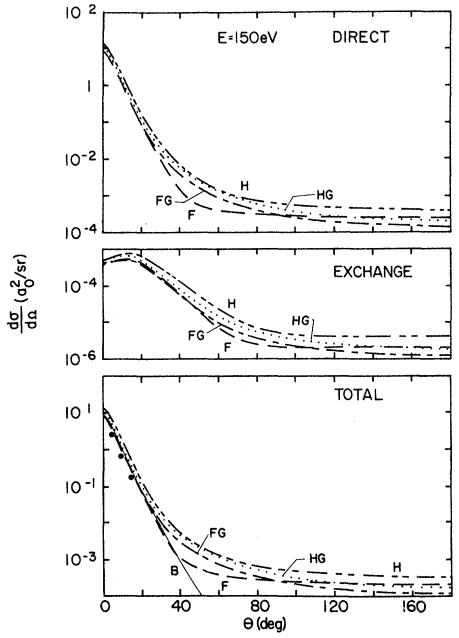

FIG. 10. Theoretical and experimental differential cross sections for electron-impact excitation of the $2\,^1P$ state of helium at an incident energy of 150 eV. The curves labeled H, HG, F, and FG are distorted-wave calculations and B is the Born approximation. A description of the distorted-wave labels is contained in Sec. III E 1. The experimental data are that of Vriens *et al.* The distorted-wave curves F and FG are identical to with in plotting accuracy in the direct and total cross sections for $\theta < 20°$.

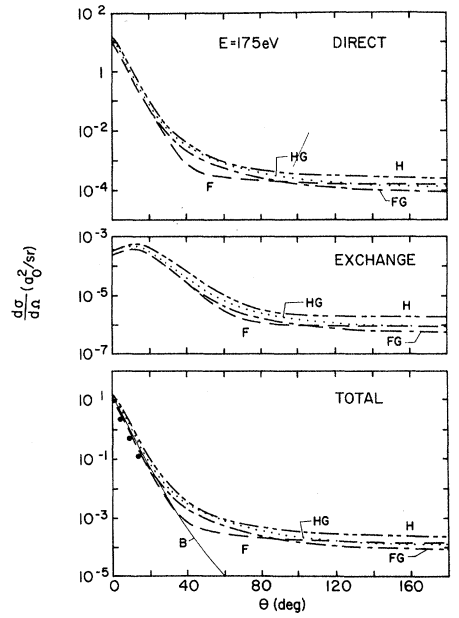

FIG. 11. Same as Fig. 10 except here the energy is 175 eV. The distorted-wave curves F and FG are identical to within plotting accuracy in the direct and total cross sections for $\theta < 20°$ and in the exchange cross section for $\theta < 45°$.

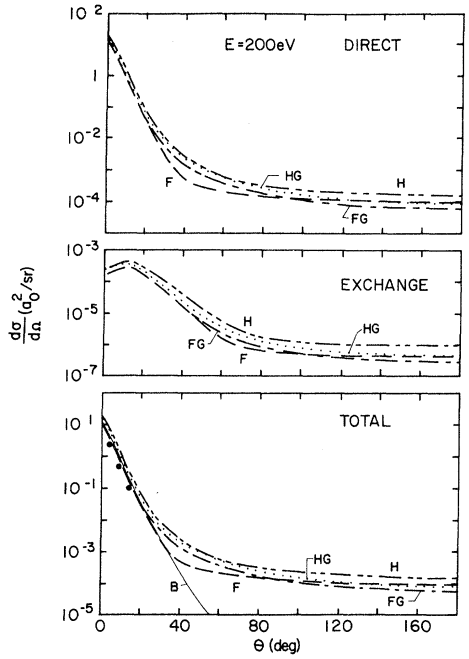

FIG. 12. Same as Fig. 10 except here the energy is 200 eV. The distorted-wave curves F and FG are identical to within plotting accuracy in the direct and total cross sections for $\theta < 20°$ and in the exchange cross section for $\theta < 45°$.

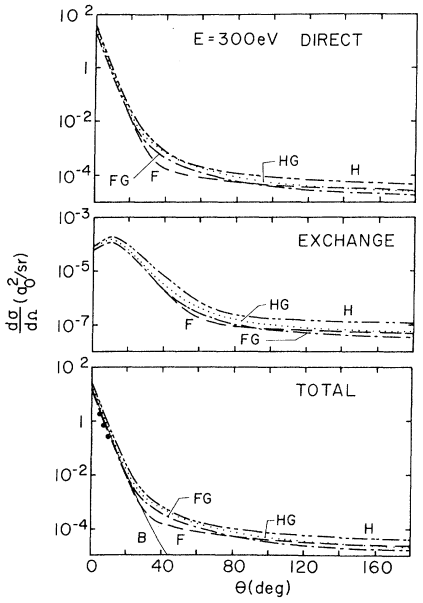

FIG. 14. Same as Fig. 10 except here the energy is 300 eV. The distorted-wave curves F and FG are identical to within plotting accuracy in the direct and total cross sections for $\theta < 20°$ and in the exchange cross section for $\theta < 40°$.

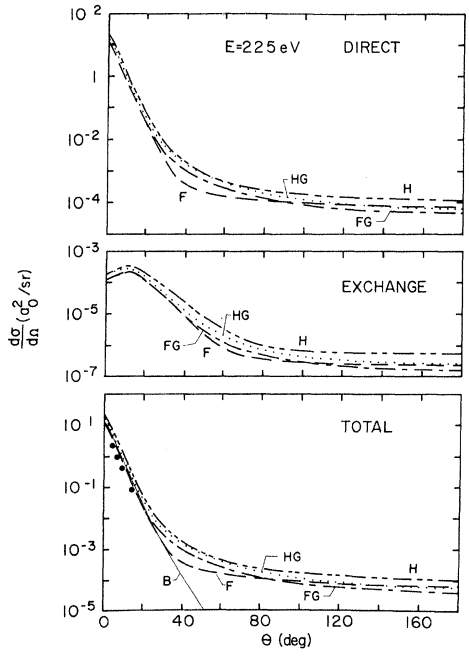

FIG. 13. Same as Fig. 10 except here the energy is 225 eV. The distorted-wave curves F and FG are identical to within plotting accuracy in the direct and total cross sections for $\theta < 20°$ and in the exchange cross section for $\theta < 40°$.

from 100 to 300 eV.

Figure 15 compares the DW calculation FG (solid line) and the Coulomb-projected Born-approximation calculation of Hidalgo and Geltman[28] (dashed line) with the experimental data of Vriens *et al.*[25] and Opal and Beaty[29] at an incident energy of 200 eV. The Coulomb-projected Born calculation is a high-energy approximation which neglects the screening effect produced by the atomic electrons, and also neglects exchange scattering which we find affects the angular distribution by about 10% at this energy. It is seen that while the Coulomb-projected Born calculation does give much improvement over the plane-wave theories, the DW calculation fits the data best at this energy.

Figure 16 gives experimental and theoretical cross sections at 5° in the energy range 50–400 eV. The theoretical values are those of the Born approximation and DW calculation FG. The experimental data are that of Chamberlain *et al.*[27] Table I gives the percentage deviation of small-angle theoretical cross sections from the experimental values of Vriens *et al.* in the energy range 100–300 eV. Figure 16 and Table I show the extent of the improvement of the DW calculations using the Fischer wave functions over the Born approximation in predicting the magnitude of small-angle differential cross sections. Both the DW and the Born calculations approach the experimental data as the energy increases. However, the FG

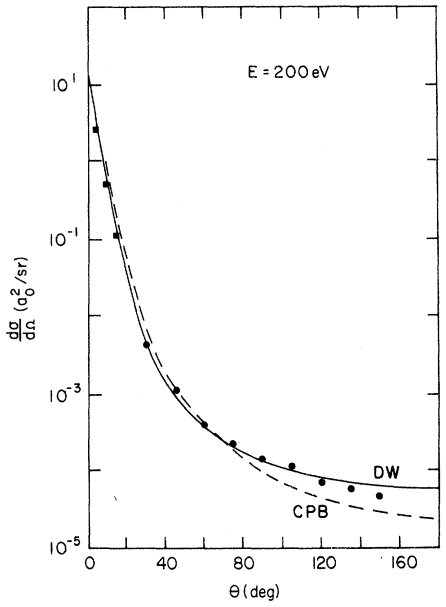

FIG. 15. Comparison of the distorted-wave calculation FG (solid line) and the Coulomb-projected Born calculation (dashed line) to the experimental data of Vriens *et al.* (solid square) and Opal and Beaty (solid circles) at an incident-electron energy of 200 eV.

calculation for 5° has already come to within the experimental error of 6% by 225 eV, while the Born calculation has come to within only 11% of the data at the higher energy of 400 eV. At 300 eV, both the shape and magnitude of the FG calculation are within experimental error.

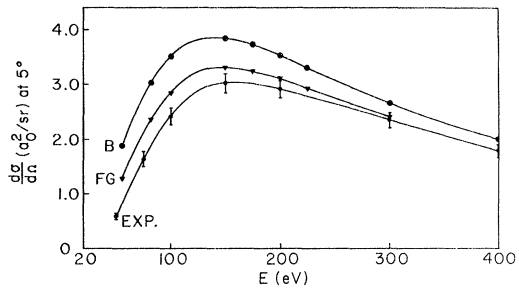

FIG. 16. Comparison of theoretical and experimental differential cross sections at 5° for the excitation of the $2\,^1P$ state of helium. The experimental data (heavy points with error bars) is that of Chamberlain *et al.* FG is a distorted-wave approximation calculation and B is a Born approximation calculation using Kim and Inokuti's generalized oscillator strengths.

Comparison of the four different DW calculations presented here reveals that they all predict a similar type of angular dependence for a given energy. The calculations using the Hartree–Fock wave functions of Fischer[33] give small-angle cross sections whose magnitude is closer to the experimental data than the calculations using the poorer wave functions of Herman and Skillman.[32] A very interesting feature is that HG and FG have almost identical shapes, and a corresponding similarity exists between H and F. Since H and F satisfy similar orthogonality conditions, as do HG and FG, this observation suggests that the shape of the cross section depends more strongly on the orthogonality conditions than it does upon the accuracy

TABLE I. Comparison of theoretical and experimental differential cross sections for the excitation of the $^1P_1$ state of helium at different impact energies.

E (eV)	θ (deg)	Expt.[a]	FG[b]	% deviation from expt.	F[c]	% deviation from expt.	B[d]	% deviation from expt.
100	5	2.411	2.837	18	2.892	20	3.509	46
	10	0.918	1.122	22	1.176	28	1.367	49
	15	0.335	0.432	29	0.459	37	0.516	54
	20	0.123	0.172	40	0.179	46	0.198	61
150	5	3.018	3.306	10	3.315	10	3.837	27
	10	0.759	0.867	14	0.899	18	0.998	31
	15	0.205	0.251	22	0.262	28	0.283	38
200	5	2.911	3.107	7	3.113	7	3.524	21
	10	0.563	0.624	11	0.647	15	0.702	25
	15	0.124	0.147	19	0.152	23	0.162	31
300	5	2.339	2.382	2	2.404	3	2.647	13
	7.5	0.821	0.853	4	0.876	7	0.947	15
	10	0.312	0.333	7	0.347	11	0.369	18

[a]Experimental values of Vriens *et al.* normalized to the absolute measurements of Chamberlain *et al.*
[b]Distorted-wave calculation using atomic wave functions of Fischer calculated in the frozen-core approximation.
[c]Distorted-wave calculation using atomic wave functions of Fischer calculated separately for each channel.
[d]Born approximation using the generalized oscillator strengths of Kim and Inokuti.

of the wave functions. It is also to be noted that the improvement of the orthogonality criterion between H and HG and between F and FG shifts the magnitude of the small-angle differential cross sections closer to the experimental data. The best fit then is obtained for FG and not for the calculation with the best bound-state wave functions F.

Massey and Mohr calculated the differential cross section for excitation of the $2\,^1P$ state of helium using a DW method with and without exchange[39] for incident energies of 33 and 50 eV. They used the simplest Hylleraas wave function for the ground state and the simplest Eckart-type wave function for the excited state. Since their calculation was not normalized, only shapes of the angular distributions can be compared. The shapes given by the present calculations fit the data better. This is not surprising when consideration is given to the wave functions they used and to the numerical approximations they were forced to make owing to the lack of modern computational machinery.

Table II examines the effect of the exchange term on the differential cross section. The exchange term decreases the magnitude of the cross section, and the values listed in the table give the percentage of the decrease. The values were obtained from the FG calculation. In general the exchange term has the largest effect for the lower energies, and for a given energy it has the largest effect for the larger angles. The increasing effect of the exchange term as θ increases from 0° to 30° brings the theoretical results into closer agreement with the data. Examination of the DW results presented here reveals that the exchange amplitude does not drastically alter the behavior of the angular distributions, in contrast to some Ochkur and Ochkur-like approximations. For incident energies greater than 55.5 eV, the exchange differential cross sections have a peak away from 0°. A similar behavior was obtained in previous calculations of the exchange amplitude with Ochkur–Bonham-like relations.[8]

TABLE II. Effect of the distorted-wave exchange amplitude on the theoretical angular distributions for the excitation of the $^1P_1$ state of helium at different impact energies. The bound-state wave functions were calculated with Fischer's program using the frozen-core approximation.

E (eV)	0°	15°	30°	60°	90°	135°	180°
34	19%	25%	38%	54%	60%	63%	59%
55.5	7%	14%	28%	35%	39%	41%	39%
100	2%	9%	21%	19%	22%	23%	23%
150	1%	8%	17%	12%	14%	15%	16%
300	0%	7%	10%	6%	7%	8%	9%

2. Integrated Cross Sections

Figure 17 compares various theoretical integrated cross sections with the experimental results of Jobe and St. John.[30] The three plane-wave curves calculated using Kim and Inokuti's generalized oscillator strengths are taken from Ref. 8. The DW curve F is not shown above 81.63 eV since it would not be distinguishable from the FG curve. On an expanded scale the F curve would lie above FG in this energy range. The DW curve H (not shown) gives integrated cross sections that are off the scale in the intermediate energy range. All the theoretical cross sections exceed the experimental data in the intermediate energy range, but the FG curve fits best. While the various plane-wave calculations appear to be approaching the experimental data at higher energies, the DW calculations using the Fischer wave functions have already come to within experimental error at about 200 eV.

As was the case for the differential cross sections, the present DW integrated cross sections do not agree with the earlier DW work of Massey and Mohr.[39] Their integrated cross section has a high maximum near 55 eV, falls rapidly, and crosses the experimental data near 100 eV. All of the present DW calculations (except H) yield a smaller maximum which occurs at a higher energy.

F. Errors

When performing a calculation such as this, a careful monitor of the numerical errors must be maintained. The errors contributing to uncertainty in the direct amplitude are errors in the DW's, numerical integration errors, and tail error. Errors in the DW's arise from using a finite number of points per lobe in the calculation of the waves, and numerical integration errors arise from the finite spacing of the integration points used in calculating the overlap integrals. Tail error is the label given to the contribution to the overlap integrals that is missed because the outward integration is terminated before the form factor has reached zero.

For the exchange case, only errors in the DW's and numerical integration errors contribute appreciably to uncertainty in the amplitude. These errors will give a larger uncertainty in the exchange amplitude than they gave in the direct amplitude since the exchange amplitude requires a larger number of numerical manipulations. This effect could be devastating to the calculation if the exchange integral had to be evaluated over the same number of integration points as the direct integral. However, since the exchange integration can be terminated when the bound-state wave function effectively vanishes, the number of integration

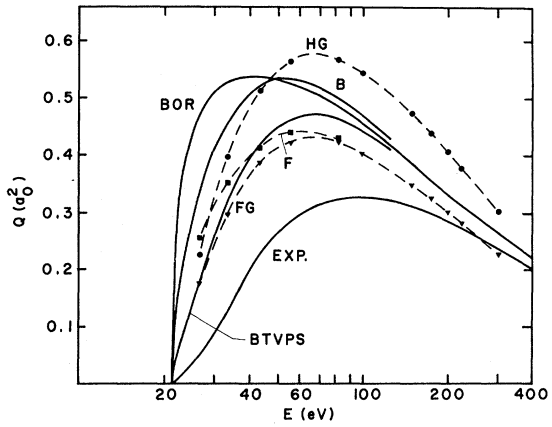

FIG. 17. Comparison of theoretical and experimental integrated cross sections for the excitation of the $2\,^1P$ state of helium. The experimental cross-section curve is that of Jobe and St. John; the plane-wave curves B, BOR, and BTVPS are those of Truhlar *et al.*, and the distorted-wave curves HG, F, and FG are from the present calculation.

points required for the exchange integral was only 200–400 (versus 1500 for the direct integral), and good accuracy was maintained.

The wave-function error and numerical-integration error were kept at one to two orders of magnitude smaller that the tail error in the direct amplitude in order than the total uncertainty be about the same in both the direct and exchange amplitudes. To meet this requirement, it was found that the DW's should have a minimum of 13 points per lobe. Numerical-integration error was generally a little smaller than the wave-function error, but they were of comparable orders of magnitude. It is worthwhile to note that the different errors affect the direct overlap integrals in basically different manners. The wave-function and integration errors tend to give a percentage error that is independent of the angular momentum of the partial wave. On the other hand, the tail error is approximately a constant, and thus yields a percentage error which increases with increasing angular momentum of the partial waves.

An error-predictor code was written for the purpose of monitoring and controlling the numerical errors. The code was tested on a calculation of the differential cross section for the excitation of hydrogen from its ground state to the $2p$ state in the Born–Oppenheimer approximation. The results were then compared with the analytic expressions given by Corinaldesi and Trainor.[40] The errors predicted by the code agreed closely with the actual error.

Table III gives the estimated errors in the FG calculation for different impact energies using the error estimation techniques. Since the differential cross section is more sensitive to errors for angles near 180°, the errors are relatively larger for such angles (see Table III). The numerical errors in the exchange amplitude had little effect on the total cross section, and even less effect on the integrated cross section.

IV. CONCLUSIONS

The DW calculations presented here give better agreement with experiment than do previous theoretical calculations for both differential and integrated cross sections in the entire energy range considered, $29.2 \leq E \leq 300$ eV. The fit to the experimental data given by the DW differential cross sections improved with increasing energy, so that the DW curve FG lies within experimental error at practically every datum point by 81.63 eV. The DW calculations gave small-angle cross sections that were closer to absolute measurements than those given by the Born approximation. But the most dramatic improvement over the plane-wave theories was obtained at large angles, where the plane-wave theories failed by several orders of magnitude. The high-energy Coulomb-projected Born calculation of Hidalgo and Geltman gave better large-angle results than the plane-wave theories. However, the DW result FG reported here fits the data best at 200 eV, the highest energy for which large-angle data are available.

While the DW integrated cross sections reported here exceeded the experimental data in the intermediate energy range, the FG calculation did fit the data better than the best previous theoretical calculation. The DW calculations made using the Fischer wave functions gave integrated cross sections that came within experimental error beyond 200 eV.

Among the various DW results, the calculations made using the better Hartree–Fock bound-state wave functions of Fischer gave cross sections whose magnitude was closer to experiment than the calculations made using the less accurate bound-state wave functions of Herman and Skillman. Improving the orthogonality requirements for a particular set of bound-state wave functions improved both the shape and magnitude of the dif-

TABLE III. Estimated numerical errors in the distorted-wave differential cross sections for the excitation of the $^1P_1$ state of helium at various impact energies. The bound-state wave functions were calculated with Fischer's program using the frozen-core approximation.

E (eV)	0°	15°	30°	60°	90°	135°	180°
34	0.0%	0.0%	0.0%	0.0%	0.0%	0.0%	0.4%
55.5	0.0%	0.2%	0.1%	0.1%	0.0%	0.2%	1.7%
100	0.0%	0.3%	0.1%	0.3%	0.0%	0.7%	5.0%
150	0.0%	0.3%	0.1%	0.4%	0.1%	1.0%	6.6%
300	0.0%	0.3%	0.2%	0.4%	0.0%	0.6%	11.0%

ferential cross sections. The shape of the differential cross sections seemed to depend more strongly on the orthogonality requirements than on the accuracy of the bound-state wave functions. The best fit to the experimental data was obtained using the better bound-state wave functions of Fischer with their accuracy somewhat reduced in favor of satisfying some of the orthogonality requirements.

The effect of the exchange term on the DW results was greatest at the lower incident-electron energies, and at a given energy it had the greatest effect at the larger angles. The exchange term lowered the magnitude of the DW results and so improved the agreement with experiment, but it did not greatly alter the behavior of the angular distributions.

The failures and successes of the plane-wave approximations can be easily understood within the framework of the DW approximation. The plane-wave approximations will give reasonable results only when the distorted partial waves can be replaced by spherical Bessel functions over the radial range where most of the contribution to the scattering amplitude is obtained. This replacement is never justified in the exchange case. In this case, the bound-state wave functions are integrated against free-state wave function [see Eq. (2)]. Thus the contribution to the exchange scattering amplitude comes from the region where the bound-state wave functions have an appreciable value. In this region the atomic potential is also large, and hence is precisely the region where distortion is most important. Consequently, the various plane-wave exchange approximations give angular distributions which disagree with one another, and which bear little or no resemblance to the experimental data.

As for the direct-scattering amplitude, the special case for which the Born approximation gives good results, i.e., for allowed transitions at high energies and small angles, is understood as being just that case for which distortion is unimportant. To see this, one must consider the radial overlap integrals of the DW approximation, which determine the cross section. The direct-scattering radial overlap integral of the DW approximation is obtained by first integrating the product of the bound-state wave functions against the radial multipole factor to yield the form factor [see Eq. (10)] which is a function of the scattered electron radial coordinate. The form factor is then integrated against the product of the initial and final distorted partial waves of the free electron. The strength of the form factor at a given radius thus controls the strength of the scattering for that radius. For the case of a dipole-allowed transition, the form factor at large r is seen to be $1/r^2$ times the dipole matrix element between the initial and final bound-state wave functions. This long-ranged form factor remains large beyond the atomic radius, so that the radial range in which distortion is small contributes strongly to the scattering and is the main contributor to the higher partial waves. The small-angle scattering results predominately from the higher partial waves (semiclassically, large impact parameters), and hence is affected only minimally by the distortion. This argument holds only at energies sufficiently high that exchange and coupling effects are negligible.

At energies near threshold and somewhat above, the DW approximation does not give the good quantitative agreement with experiment that it gives at higher energies. At these lowest energies one is forced to resort to the close-coupling, correlation, or some other elaborate method. The upper limit in energy of a few keV at which the DW approximation may be applied routinely is governed by the limitations of present-day computers. At these high energies the analytical Coulomb-projected Born approximation is expected to give good results, but further comparisons with high-energy angular distribution data are needed to establish the validity of this approximation. The region in which the DW approximation is highly useful is the intermediate energy range where there formerly existed no valid calculations of angular distributions.

The reader will note that we have not displayed generalized oscillator strengths. It is well known that the Born approximation gives generalized oscillator strengths which depend only on the transferred momentum, and not on the energy. The usefulness of the generalized oscillator-strength concept depends on this latter property which incorporates the scattering at all energies into a single generalized oscillator-strength curve. Therefore, this concept is useful only for the limited special cases in which the Born approximation gives good results. Accordingly, we have refrained from extracting "apparent generalized oscillator strengths" from our DW differential cross sections. Generalized oscillator strengths extracted in this way either from our DW theoretical results or from experiment depend on the energy as well as the momentum transfer. It thus seems more sensible to display the differential cross sections directly, rather than to display a derived indirect quantity to which no particular advantage is attached.

It might appear that it would have been desirable to have performed a calculation using highly accurate correlated bound-state wave functions. However, the results of this paper show that it is useless to employ highly accurate bound-state wave functions in a first-order or modified-first-order scattering calculation, except for the special case

in which the scattering part of the calculation may be done crudely, i.e., for high energies and small angles. In consideration of this latter case, we point out that a DW calculation using correlated wave functions is beyond our present computational resources.

A brief report[41] on this work was given at the Seventh International Conference on the Physics of Electronic and Atomic Collisions.

It was not feasible to include in tabular form all the DW numerical results presented in the present work. Complete tables for the FG calculation may be obtained from one of the authors (W. N. S.).

The reader may find of interest some recent work on the excitation of the $2\,^1P$ state of helium calculated in the eikonal approximation by Byron.[42] Unfortunately, the numerical errors in his calculation preclude a meaningful comparison with the present calculation. (See Fig. 1 of his work.)

ACKNOWLEDGMENTS

The authors give thanks to J. Mazeau for making his unpublished angular distribution data available, to C. B. Opal and E. C. Beaty for sending their unpublished large-angle data, to M. B. Hidalgo and S. Geltman for sending the results of the Coulomb-projected Born calculations prior to publication, and to G. B. Crooks and M. E. Rudd for sending their unpublished data.

---

*Work supported in part by the National Science Foundation under Grant No. GJ365.

[1]M. Born, Z. Physik 38, 803 (1926).

[2]H. Bethe, Ann. Physik 5, 325 (1930).

[3]J. R. Oppenheimer, Phys. Rev. 32, 361 (1928).

[4]R. H. Bonham, J. Chem. Phys. 36, 3260 (1962).

[5]H. M. Mittleman, Phys. Rev. 126, 373 (1962); Phys. Rev. Letters 9, 495 (1962).

[6]V. I. Ochkur, Zh. Eksperim. i Teor. Fiz. 45, 734 (1963) [Sov. Phys. JETP 18, 503 (1964)].

[7]M. R. H. Rudge, Proc. Phys. Soc. (London) 85, 607 (1965); 86, 763 (1965).

[8]D. O. Truhlar, J. K. Rice, A. Kuppermann, S. Trajmar, and D. C. Cartwright, Phys. Rev. A 1, 778 (1970).

[9]L. Vainshtein, V. Opykhtin, and L. Presnyakov, Zh. Eksperim. i Teor. Fiz. 47, 2306 (1964) [Sov. Phys. JETP 18, 1383 (1964)].

[10]O. Bely, Nuovo Cimento 49, 66 (1967).

[11]W. N. Shelton, E. S. Leherissey, and D. H. Madison, Phys. Rev. A 3, 242 (1971).

[12]J. C. Steelhammer and S. Lipsky, J. Chem. Phys. 53, 4112 (1970).

[13]S. Trajmar, J. K. Rice, and A. Kuppermann, Advan. Chem. Phys. 18, 15 (1970).

[14]T. Sawada, J. E. Purcell, and A. E. S. Green, Phys. Rev. A 4, 193 (1971).

[15]W. N. Shelton and E. S. Leherissey, J. Chem. Phys. 54, 1130 (1971); a more detailed treatment of the theory is found in D. H. Madison and W. N. Shelton, Electron Physics Technical Report No. 9 (Department of Physics, Florida State University, Tallahassee, 1971) (unpublished).

[16]All equations are given in atomic units; in particular the unit of length is $a_0 = 0.529$ Å and the unit of energy is Ry = 13.605 eV.

[17]G. R. Satchler, Nucl. Phys. 55, 1 (1964).

[18]M. E. Rose, *Elementary Theory of Angular Momentum* (Wiley, New York, 1967), Chap. 3.

[19]D. M. Brink and G. R. Satchler, *Angular Momentum* (Oxford U. P., London, England, 1968), Chap. 3, p. 45.

[20]Reference 19, Chap. 3, p. 40.

[21]Reference 19, Chap. 5, p. 83.

[22]A. de-Shalit and I. Talmi, *Nuclear Shell Theory* (Academic, New York, 1963), Chap. 31.

[23]L. J. Keiffer, *Bibliography of Low Energy Electron Collision Cross Section Data*, Natl. Bur. Std. (U. S.) Misc. Publ. No. 298 (U.S. GPO, Washington, D.C., 1967).

[24]B. L. Moiseiwitsch and S. J. Smith, Rev. Mod. Phys. 40, 238 (1968).

[25]L. Vriens, J. A. Simpson, and S. R. Mielczarek, Phys. Rev. 165, 7 (1968).

[26]Y. K. Kim and M. Inokuti, Phys. Rev. 175, 176 (1968).

[27]G. E. Chamberlain, S. R. Mielczarek, and C. E. Kuyatt, Phys. Rev. A 2, 1906 (1970).

[28]M. B. Hidalgo and S. Geltman, J. Phys. B 5, 617 (1972).

[29]C. B. Opal and E. C. Beaty, J. Phys. B 5, 627 (1972).

[30]J. D. Jobe and R. M. St. John, Phys. Rev. 164, 117 (1967).

[31]R. W. La Bahn and I. Callaway, Phys. Rev. 180, 91 (1969).

[32]F. Herman and S. Skillman, *Atomic Structure Calculations* (Prentice-Hall, Englewood Cliffs, N. J., 1963).

[33]C. Froese Fischer, Computer Phys. Commun. 1, 151 (1969).

[34]W. N. Shelton, K. L. Baluja, and C. E. Watson, J. Phys. B 4, 71 (1971).

[35]J. M. Blatt, J. Computational Phys. 1, 382 (1967).

[36]R. W. Southworth and S. L. Deleeuw, *Digital Computation and Numerical Methods* (McGraw-Hill, New York, 1965), p. 372.

[37]J. Mazeau (private communication).

[38]G. B. Crooks and M. E. Rudd, Bull. Am. Phys. Soc. 17, 131 (1972); and private communication.

[39]H. S. W. Massey and C. B. O. Mohr, Proc. Roy. Soc. (London) A139, 187 (1933); see also S. Khashba and H. S. W. Massey, Proc. Phys. Soc. (London) 71, 548 (1958).

[40]E. Corinaldesi and L. Trainor, Nuovo Cimento 9, 940 (1952).

[41]D. H. Madison and W. N. Shelton, in *Proceedings of the Seventh International Conference on the Physics of Electronic and Atomic Collisions*, edited by L. M. Branscomb, R. Geballe, F. J. deHeer, N. V. Fedorenko, J. Kistemaker, M. Barat, E. E. Nikitin, and A. C. H. Smith (North-Holland, Amsterdam, 1971), pp. 768–770.

[42]F. W. Byron, Jr., Phys. Rev. A 4, 1907 (1971).